Applied Environmental Research
- RESEARCH FOR SUSTAINABLE PLANET -

Research Article

Analyzing Climate Change Status through Evaluating Trend of Temperature and Rainfall and Predicting Future Climate Change Status at Lake Tana Basin

Tesfaye Bayu[1,2,*], Tri Retnaningsih Soeprobowati[2,3], Solomon Adissu[4]

[1] Debre Markos University, Burie campus, Burie, Ethiopia
[2] School of Postgraduate Studies, Universitas Diponegoro, Semarang, Indonesia
[3] Department of Biology, Faculty of Science and Mathematics Universitas Diponegoro, Semarang, Indonesia
4 Bahir Dar University, collage of agriculture and environmental science, Ethiopia

*Correspondence Email: tesfayebayu235@gmail.com

Abstract

The trends of temperature and rainfall are critical indicators of climate change within a certain area. However, the existence of climate change is not locally understood in most parts of the world. This research aims to analyze the trend of temperature and rainfall in the Lake Tana Sub-basin as a means to understand the current and future status of climate change. The trends of temperature and rainfall were analyzed using the modified Mann-Kendall trend test, while the autoregressive integrated moving average model (ARIMA) was used to predict future temperature and rainfall. The findings reveal that monthly temperatures show a significant increasing trend for March, April, May, June, and December with Z-values of 3.96, 3.32, 2.64, 3.21, and 4.6, respectively. Seasonal and annual temperatures also show a significant increasing trend with Z-values of 4, 5.35, 5.08, and 4.41 for spring, autumn, winter, and annual, respectively. The Mann-Kendall trend analysis results show that monthly, seasonal and annual rainfall exhibit significant increasing trends for some months and seasons. The results of the ARIMA model suggest that the predicted values of temperature and rainfall will continue to increase over the next 10 years in the study area. Based on these findings, it can be concluded that there is a significant and increasing trend in temperature and rainfall, which will likely continue over the next decade, indicating the presence of climate change in the study area. The research findings suggest that temperature and rainfall have been increasing over time, leading to climate change in the study area, so sustainable lake management and urban development should be practiced to mitigate and adopt climate change.

ARTICLE HISTORY
Received: 4 Jul. 2023
Accepted: 5 Jan. 2024
Published: 6 Mar. 2024

KEYWORDS
Climate change;
Rainfall trend;
Temperature trend;
Temperature prediction

Introduction

Climate change is primarily caused by human activities as well as natural processes, resulting in rising average temperatures, increased variability of rainfall frequency and intensity, increased atmospheric greenhouse gas concentrations, increased frequency and severity of storms, and rising sea levels [1]. Temperature and rainfall fluctuations are widely recognized as indicators of climate change and variability across the globe, as noted by IPCC [2].

Ongoing climate change has caused a significant increase in the global land surface temperature, by 0.99 ◦C from 1850–1900 to 2001–2020, with recent decades being progressively warmer than previous ones, as reported by IPCC [2]. The mean temperature trend can be attributed to either the maximum temperature or minimum temperature trend, or both, as noted by Qu et al. [3]. Global air surface temperatures have risen by an average of 0.85°C since 1880, surpassing the rates of previous centuries [4]. Future temperature predictions

https://doi.org/10.35762/AER.2024003

suggest that this warming trend will persist throughout the remainder of the 21st century, with subarctic and arctic regions experiencing even greater warming than global averages [5]. As Luoto and Nevalainen [6] explain, water temperature is closely linked to air temperature and solar radiation. Therefore, increasing air temperatures result in higher freshwater temperatures. In fact, Holsinger et al. [7] found that mean annual water temperatures have increased by 0.3°C per decade worldwide during the 20th century. In fact, during the past century, there has been a significant increase in atmospheric CO_2 concentration, resulting in a rise of the mean global temperature by 0.74°C compared to preindustrial times [8].

Most parts of Sub-Saharan Africa (SSA) are likely to experience a decrease in precipitation amounts while rainfall variability is expected to increase [9]. Chinwe [10] has argued that Africa is particularly vulnerable to negative impacts of climate change such as high temperatures and unpredictable rainfall, given its status of wide-spread poverty and low development. To support agro physical modeling, it is crucial to predict the future meteorological quantities based on historical time series [11].

Ethiopia is a country that is particularly vulnerable to the impacts of climate change [12]. Notably, since the 1990s, Ethiopia has been experiencing an annual temperature increase of 0.37°C per decade. It is anticipated that this trend will continue, with projected temperature increases of 0.9 to 1.1°C, 1.7 to 2.1°C, and 2.7 to 3.4°C by 2030, 2050, and 2080, respectively, when compared to the temperature status during the period from 1961–1990 [12].

While some studies have focused on changes in global and regional mean temperature, others have examined temperature trends on different spatial and temporal scales [13]. The majority of these studies have found that temperatures are increasing, though variations differ by region [14]. In Nigeria, the general trend of both minimum and maximum temperature was found to be increasing [15].

A newly emerging technique to design new strategies for climate change mitigation and adaptation involves understanding the status of climate change by analyzing trends in temperature and rainfall in a given area [16]. In areas such as those surrounding large water bodies like Lake Tana, climatic variables are particularly fragile, making analysis of major climatic variables crucial in predicting the status of climate change [17]. Rather than using climate change prediction models applied by researchers from other areas, this research analyzed the trend of temperature and rainfall to understand the status of climate change in the study area and forecasting future climate change trend [18]. This approach is unique and not explored by other scholars. Due to global warming, higher temperatures and limited precipitation can cause drought, which poses a serious threat to food security [19].

Numerous time series forecasting methods rely on analyzing past data to forecast future events [20]. These models are based on the assumption that past patterns can be used to predict future patterns [21]. In this study, the researchers utilized Autoregressive integrated moving-average to forecast future temperature and rainfall patterns in the Lake Tana sub basin. Autoregressive integrated moving-average (ARIMA) modeling is a popular method for time series modeling, which carefully examines past observations of a time series to develop an appropriate model to forecast future values [22].

The significance of this research paper lies in its innovative approach to assessing climate change and forecasting future climate patterns in the Lake Tana sub-basin. By analyzing temperature and rainfall trends, the authors aim to identify and understand the presence of climate change in the region, which has not been explored by other scholars previously. This finding holds great importance as it highlights the potential risk of drought due to global warming, higher temperatures, and limited precipitation, thereby posing a serious threat to food security. The research indicates the need for the design and implementation of effective mitigation and adaptation measures to address the challenges posed by climate change in the Lake Tana sub-basin.

Climate change affects areas which are near to lakes and climatic variables of the study area were highly fluctuating due to climate change. That is why the research was imitated with objective of to analyze the trend of temperature and rainfall in the Lake Tana Sub-basin as a means to understand the current status of climate change. Furthermore, the study aims to forecast future climate change patterns in the area using the ARIMA model, departing from the commonly used climate change prediction models applied by researchers from other regions. This unique approach provides valuable insights into the climate dynamics specific to the study area. These objectives provide comprehensive insights into the current and future climate change scenario, enabling policymakers, researchers, and communities to formulate appropriate strategies and interventions to mitigate the adverse effects of climate change and ensure sustainable development in the region.

Description of study area

The research site is situated in the Amhara National Regional State, specifically in the Lake Tana Sub-basin

(LTSB) of the Blue Nile Basin. The Blue Nile Basin is recognized as the largest river basin in Ethiopia and comprises the LTSB, home to the world's largest freshwater and oligotrophic-high altitude lake, Lake Tana [23]. The area covers a total land area of 1,589,654.98 hectares in the upper reaches of the Blue Nile River [23]. The atmospheric temperature at Lake Tana sub basin typically falls between 13 and 22°C, with a decrease of 0.7°C per 100 m in elevation [24]. Located geographically in the range of 10°45054.1" N, 36°10024.9" E and 12°50015.9" N, 38°50054.48" E (Dersseh et al., 2019), Lake Tana experiences an average annual rainfall of 1248 mm per year (mm yr^{-1}). This represents a 7% reduction in rainfall when compared to the surrounding watershed.

The Lake Tana basin is mainly characterized by cultivable land, which accounts for 71% of the area, followed by grazing land (9%), infrastructure (6%), forestland (3%), and other types of land. The major land cover types include farmland, water bodies, wetlands, forests, woodlands, shrubs, rangeland, grassland, and settlements. The dominant soil types on Lake Tana's islands, peninsulas, wetlands, and upland areas are Nitosols, Luvisols, and Vertisols [24].

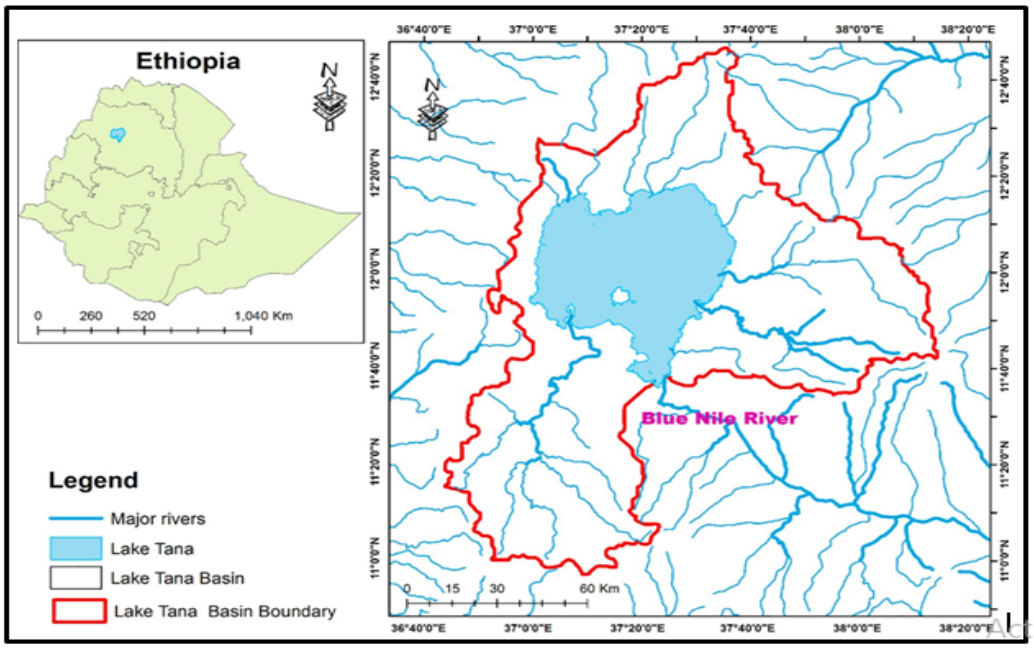

Figure 1 Map of the study area.

Method

1) Data type and sources

This research utilized both primary and secondary data sources. The primary data was obtained by observing climatic variables from metrological stations located in the study area, including Zega, Bahir Dar, Delgi, Deke Stifanos, and Chawhit stations. These stations were used to check, validate, and calibrate the secondary data sources. On the other hand, 30 years of temperature, rainfall, and humidity data from the NASA database were downloaded for the purpose of analyzing climate change. The decision to use the NASA database was based on its accessibility and credibility as a source of updated and reliable data.

2) The climate database

To describe the existing climate conditions in the research area, two bioclimatic variables were extracted from the latest NASA database [26]. The data falls into three categories and was fine-tuned by combining local observations with the site-specific information collected from five metrological stations situated in the vicinity. This dataset encompasses different climatic parameters, such as yearly means, seasonal variations, and monthly extreme values, for rainfall, and temperature in the Lake Tana sub basin.

3) Data collection and processing

To analyze the trend of climatic variables in the study area, daily data on minimum and maximum temperature, and rainfall were obtained from meteorological stations. The historic data on temperature, and rainfall were collected from five stations, namely Zega, Bahir Dar, Delgi, Deke Stifanos, and Chawhit, for the period of 1990 to 2020 (NY=30). Both primary and secondary data sources were utilized to achieve objective of the research. The collected data was utilized for the analysis of the trend of climatic variables in the study area. The study area utilized climatic data from the NASA database spanning a period of thirty years, specifically from 1990, 2010, and 2020. The data encompassed information on temperature, and rainfall. Calibration

of the data was subsequently conducted by gathering meteorological data on rainfall, and temperature, from five nearby stations. These data were then used for both the calibration and validation of the NASA climatic data base for the study area. The data extracted from NASA was used for trend analysis since the reading is not deviated from satiation reading.

4) Data quality control

To ensure the quality and reliability of the data, both visual and statistical assessments were conducted. In the visual assessment, temperature, and precipitation data were carefully screened for any outliers or missing values that could potentially skew the final results. Statistical testing was performed using the Mann-Kendall test method, preceded by a trend-free pre-whiting process and variance correction approaches to minimize the impact of serial correlation in the data [27]. Data homogeneous analysis was done by conduction autocorrelation. The data was significant that is why Mann-Kendall test was conducted.

5) Data analysis

This study performed a time-series multi-temporal analysis of climatic elements recorded within the study area. The collected data on climatic variables underwent a descriptive statistical analysis, which provided annual and monthly mean values of each variable. Climatic data were obtained from both the NASA climatic database and meteorological stations situated within the study area. Standard deviation was employed to verify the accuracy of the obtained data. To address any missing data, interpolation techniques were applied based on the approach described by [28]. Specifically, the interpolation method utilized data from neighboring years that had a difference of 5 years for accurate estimation.

The R software package (R 4.3.0 version) was employed to analyze the trends of climatic elements between 1990 and 2020. This program is highly regarded for data analysis due to its capacity to produce high-quality results, which are highly acceptable for publication. To address missing data, interpolation techniques and data-cleaning processes were carried out. Significant differences among each climatic element were examined with the use of the R software package. Additionally, regression analysis was employed to develop a model for predicting and extrapolating the values of the climatic elements.

6) Modified Mann–Kendall climatic variable trend test

Modified Mann–Kendall trend test is a non-parametric test which was used to identify a trend in a series of climatic variables. It was used to determine whether a time series has a monotonic upward or downward trend for climatic variables for long period of time. There are two benefits of using this test. First, it does not require the data to be normally distributed since the test is non-parametric (distribution-free test) and second, the test has low sensitivity to abrupt breaks due to inhomogeneous time series. The data values were evaluated as an order time series and all subsequent data values were likened from each data value. The time series x1, x2, x3… xn represents n data points. Modified Mann–Kendall trend test was used due to the data was non parametric. It's also used because of the data is not normally distributed.

The MK test statistic (S) was calculated as follows:

$$S = \sum_{i=1}^{n-1} * \sum_{j=i+1}^{n} \sin(xj - xi) \quad \text{(Eq. 1)}$$

Where

$$\text{Sin}(x) = \begin{cases} 1 \text{ if } x>0 \\ 0 \text{ if } x=0 \\ -1 \text{ if } x<0 \end{cases} \quad \text{(Eq. 2)}$$

If S>0, then it was an indicator of an increasing trend in climatic variable(x), while the reverse is true if S<0 will show decreasing trend in climatic variable(x), while S=0 indicates neither decreasing nor increasing in climatic variable(x) for long climatic time series data.

The mean of S is E[S] =0 and the variance (2) of S was given by:

$$\sigma^2 = \frac{1}{18}\{n(n-1)(2n+5) \sum_{j=1}^{p} tj\,(tj-1)(2tj+5)\} \quad \text{(Eq. 3)}$$

Where p is the number of tied groups in the time series climatic data and tj is the number of data points in the jth group.

The statistic S is approximately normally distributed provided that the following Z-transformation was employed:

$$Z = \begin{cases} \frac{s-1}{\sqrt{\sigma^2}} \text{ If } S>0 \\ 0 \text{ if } S=0 \\ \frac{s-1}{\sqrt{\sigma^2}} \text{ If } S<0 \end{cases} \quad \text{(Eq. 4)}$$

The normal approximation test is used for datasets with more than ten values, provided that there aren't many tied values within the set. If there is no monotonic trend (i.e., the null hypothesis) in climatic time series with more than ten elements, then z ~ N(0,1). This means that z follows a standard normal distribution. The probability density function for a normal distribution with a mean of 0 and a standard deviation of 1 is given by the following equation:

$$F(x) = \frac{1}{\sqrt{2\pi}}(e)^{\frac{-8}{2}} \quad \text{(Eq. 5)}$$

All the above procedures used to compute the modified Mann– Kendall Trend test were collected and referenced from [29]. In order to say the trend was increasing or decreasing the p value (>0.05) was used as comparison of Z value. If values were above 1.96 the trend was positive and increasing.

7) Sen's slope estimator and percentage change

In the event of a linear trend in the time series, the actual slope was measured using Sen's slope method, a basic non-parametric test. Sen [30] created the non-parametric technique to compute the slope of the trend in a sample of N data pairs. Additionally, it indicates the dependent variable's rate of change due to the independent variable. As the rate of change increase (Sen's slope) the Z value (MK trend test) was high and show increasing trend.

$$Ti = \frac{xj-xk}{j-k} \text{ for } i=1, 2, 3 \ldots N \quad \text{(Eq. 6)}$$

Where Xj and Xk represent the data value at the time-steps 'j' and 'k' with 'j' correspondingly greater than 'k'. The median of these 'N' values of Ti is termed as Sen's estimator of slopes and is calculated by the following formulae:

$$\beta = \frac{1}{2}\left(\frac{TN}{2} - \frac{TN+2}{2}\right) \text{ if N is even} \quad \text{(Eq. 7)}$$

$$\beta = \left(\frac{TN+1}{2}\right) \text{ if N is odd} \quad \text{(Eq. 8)}$$

The number of observation for this research was 30 which are odd. Therefore, the second formula was used to calculate Sen's slope.

8) The ARIMA model for forecasting future temperature and rainfall trend

Autoregressive integrated moving average (ARIMA), also known as Box-Jenkins models, are generated by differencing a non-stationary time series and then fitting an autoregressive moving average (ARMA) model to the resulting series. ARIMA was used due to its prediction was strong and it is in line with the prediction conducted by IPCC and the model was automatic is easily integrated with R studio to conduct prediction.

Consider the time series yt, the first difference is given by

$$Y_t - y_{t-1} = (1-B)y_t \quad \text{(Eq. 9)}$$

Where B is the backshift operator defined as $B^j y_t = y_{t-1}$ Hence, the d^{th} difference is therefore given as $(1-B)^d y_t = \Delta^d y_t$ and if the original series is differenced d times before fitting an ARMA(p, q) process, then the model for the original undifferenced series is said to be an ARIMA (p,d,q) generally defined as

$$W_t = \phi_1 w_{t-1} + \ldots\ldots + \phi_p w_{t-p} + \theta_1 \varepsilon_{t-1} + \ldots\ldots \theta_q \varepsilon_{t-q} \quad \text{(Eq. 10)}$$

Where $W_t = \Delta^d y_t$ the dth differences of the original series, $\phi_1 \ldots \phi_p$ are the AR parameters to be estimated and $\theta_1 \ldots \theta_q$ are the MA parameters to be estimated. As can be observed, an ARIMA (p,d,q) process is the dth differences of the original nonstationary series having p autoregressive terms and q moving average terms.

The least squares regression is applied in the estimation of ϕ abnd θ by first replacing the unobserved quantities ε_{t-1} abnd $\theta_q \varepsilon_{t-q}$ by estimated values, $\hat{\varepsilon}_{t-1}$ abnd $\hat{\varepsilon}_{t-q}$. The parameters ϕ abnd θ are then estimated by regressing Y_t on $y_{t-1} \ldots y_{t-q}$, $\hat{\varepsilon}_{t-1} \ldots \hat{\varepsilon}_{t-q}$. $\Psi_i \tilde{y}_{t-1}$

The forecast model (ARIMA) for yt+k is as follows:

$$\tilde{y}_t(k) = \sum_{i=1}^{p+d} \Psi i \, \tilde{y}t - i(k) + \hat{\varepsilon}t(k) + \sum_{n=1}^{\infty} \theta i \, \tilde{y}t - i(k) \quad \text{(Eq. 11)}$$

Result and discussion

1) Monthly temperature trend

The study has indicated that the monthly temperatures in the area exhibit both positive and negative trends over time. The month of March, April, May, June, and December showed a significant increase in temperature (p-value < 0.05), with Z values of 3.96, 3.32, 2.64, 3.21, and 4.6, respectively (Table 1). However, for the other months, i.e., February, July, August, September, October, and November, an increasing trend was found, but the Z value for the MK test is not statistically significant. The first month of the year, January, displayed a decreasing trend in temperature as indicated by the negative value obtained from the MK test (Table 1). March had the highest rate of change in temperature, with the highest Sen's slope of 0.215.

Table 1 MK trend test, Sens slope and descriptive statistics for monthly, seasonal and annual temperature

	Z-Value	Sen's slope	Minimum	Maximum	Mean	SD	CV
January	-0.62	-0.013	18.80	32.70	22.786	4.12	0.18
February	0.99	0.04	20.51	33.08	23.91	3.18	0.13
March	3.96***	0.215	23.32	38.96	28.51	4.51	0.16
April	3.32**	0.059	22.54	37.80	27.56	4.06	0.15
May	2.64**	0.191	20.63	35.63	25.898	3.87	0.15
June	3.21**	0.108	19.09	27.26	21.459	1.92	0.09
July	1.33	0.029	16.41	22.93	18.03	1.21	0.07
August	0.28	0.004	16.56	20.71	17.619	0.77	0.04
September	0.73	0.006	17.33	19.88	18.11	0.46	0.03
October	1.11	0.007	16.44	18.43	17.525	0.42	0.02
November	0.88	0.016	15.19	19.27	17.2	0.86	0.05
December	4.6***	0.199	17.60	32.02	23.716	4.78	0.20
Spring	4.00***	0.2	22.31	37.46	27.33	3.89	0.14
Summer	1.67	0.03	17.80	21.88	19.04	1.03	0.05
Autumn	5.35***	0.16	17.24	22.24	19.33	1.64	0.08
Winter	5.08***	0.28	19.18	28.81	23.32	3.17	0.14
Annual	4.41***	0.09	21.86	21.86	21.86	21.86	21.86

December had the highest Z value, whereas May had the lowest. This could be due to cloud accumulation in other months, which decreased surface temperature readings rather than increasing surface heat in the study area (Table 1). These findings are similar to those of Murat [11], who found a significant and highest variation of Z value for temperature in the Western Black Sea region of Turkey. The hottest month in the study area was March 2020, with a maximum temperature of 38.96°C. On the other hand, the coolest month was July, with a minimum temperature of 15.19°C (Table 1). The temperature variations across the months indicate the presence of climate change and variability in the study area.

In Table 1, December had the highest coefficient of variation (CV) at 20%, followed by January with 18%, March with 15%, April with 15%, and May with 15%. December also had the highest CV for temperature, indicating a mean temperature of 23.72°C, while March had the highest mean temperature and was identified as the hottest month in the study area. On the other hand, October had the lowest CV and was the coldest month, with the lowest temperature recorded at 17.2°C.

The study area exhibited a positive and increasing rate of change (Sen's Slope) in monthly temperature, with March recording the highest rate of change at 0.215, followed by December at 0.199, and May at 0.191 (Table 1 and Figure 2). Although Table 1 shows variability in the rate of change, all months recorded an increasing rate except for January, which showed a decreasing rate of monthly temperature due to a negative value of Sen's slope. Figure 3 depict random, seasonal, and trend components of temperature that demonstrate an increasing trend in every aspect. This increase in temperature may be attributed to the surface temperature rise and cloud distribution variability in the sub-basin, ultimately causing climate variability and change.

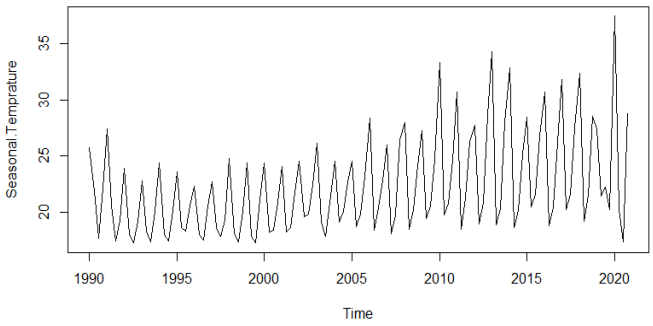

Figure 2 Trend of monthly temperature in the study area.

2) Seasonal temperature trend

The study conducted an analysis of the seasonal temperature trends in the Lake Tana Sub-basin region over a long time series of 31 years (1990 to 2020). The results of the MK trend test revealed a positive and highly significant increasing trend with Z-test values of 4, 5.35, and 5.08 for spring, autumn, and winter, respectively. While summer recorded a positive increasing trend, it was not statistically significant, with a Z-test value of 1.67 (Table 1). These results indicate an increasing seasonal temperature from time to time at p value (>0.05), as the MK trend test Z values were greater than the test statistics value (1.96) for most seasons over the last 31 years (Table 1).

Table 1 shows that spring and winter have the highest coefficient of variation (CV) of 14%, followed by autumn with 8%, and summer with 5%. The season with the highest mean seasonal temperature (27.33°C) was observed in spring. This indicates that the high CV seasons are expected to have the maximum temperature per year. On the other hand, wet seasons with fluctuating temperatures in the Lake Tana Sub-basin region have the lowest CV and reliable rainfall. The season with the lowest CV was summer, which is also the rainy season in the study area. The time series plot depicted in Figure 4 indicates that the seasonal temperature in the sub-basin has shown an increasing trend in a random, seasonal, and observed manner. This increasing trend indicates variability and changing climate in the study area.

3) Annual temperature trend

The computed p-value for the annual temperature in the basin was lower than the significance level alpha=0.05, indicating a statistically significant positive trend. This is consistent with Table 1, where the Z value (4.41) is greater than the alpha value (1.96). Additionally, the Sen's slope of the MK analysis was 0.09, demonstrating an increasing rate of temperature in the study area. Figure 5 demonstrates that, with the exception of a few years (1990, 2015, and 2020), the annual temperature in the sub-basin exhibits linear increases. The majority of the annual temperature readings are clustered near the linear line, indicating a gradual increase in temperature over time in the study area.

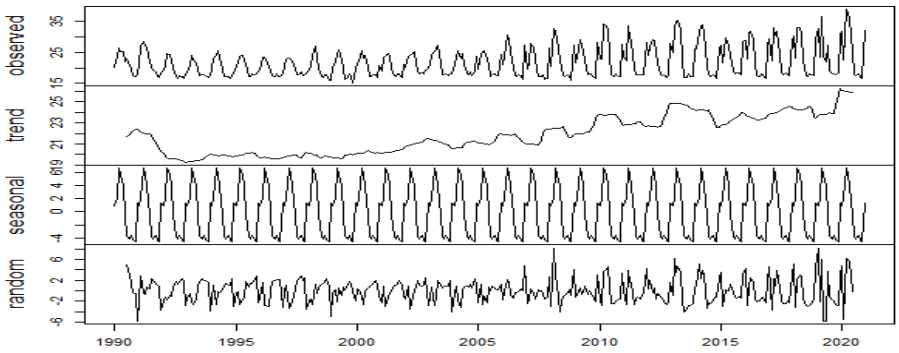

Figure 3 Comparison of seasonal, observed and random trend of monthly temperature.

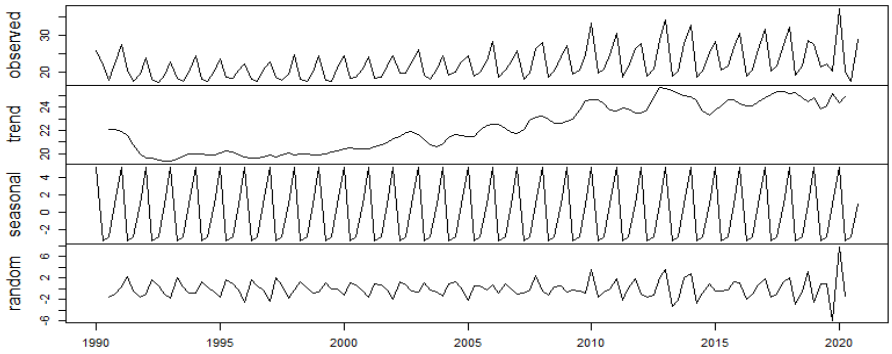

Figure 4 Comparison of observed, random and seasonal temperature in the study area.

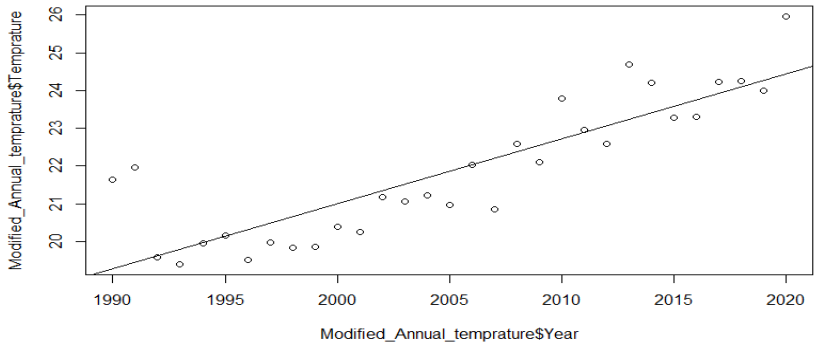

Figure 5 Annual temperature trend of the study area.

4) Monthly rainfall Trends

In this study, the Mann-Kendall test was employed to investigate rainfall trends across various time scales in the Lake Tana sub-basin. Long-term rainfall data were collected and analyzed, as shown in Table 1. The calculated value of Z1-/2 at a 95% confidence level is

equal to 1.96, which serves as the standard normal variant. Z-values in Table 1 exceeded this value, indicating that significant trends were detected in the sub-basin's monthly rainfall time series.

Table 1 also revealed positive and negative values for Z and Sens slope (β), respectively. Four months (January, March, April, and December) demonstrated decreasing trends in monthly rainfall time series data, while the remaining eight months showed an increasing trend in the study area. The Sens slope β varied from -0.01 mm/year in March and April to 0.0 mm/year in January and December.

Table 2 indicates that significant increasing trends were observed for monthly precipitation in May, July, August, September, and October, with higher Z-values compared to other months. In contrast, for February, June, and November, the Z-value was positive, indicating a simple increasing trend without significant change. The β values for May, July, August, September, and October were 0.09, 0.15, 0.14, 0.07, and 0.19 mm/year, respectively (Table 2).

According to Table 2, December had the highest coefficient of variation (CV) at 133%, followed by January with 118%, and February with 116%. November had a CV of 91%, and March had a CV of 71%. These results suggest that the five high CV months are expected to receive low annual rainfall amounts. Notably, these months are part of the dry season in the Lake Tana Sub-basin and are considered the most unreliable rainfall months. On the other hand, June, July, August, September, May, and April had the lowest CV values. These six months were associated with high rainfall over the Lake Tana Sub-basin during the study period. These findings indicate that the six months with the lowest CV values represent the wet season months in the Lake Tana Sub-basin (Table 2).

Table 2 MK trend test, Sens slope and descriptive statistics for monthly, seasonal and annual rainfall

	Z-Value	Sen's Slope	Minimum	Maximum	Mean	SD	CV
January	-0.68	-0.003	0	0.97	0.19	0.23	1.18
February	1.57	0.005	0	1.49	0.327	0.38	1.16
March	-0.54	-0.011	0.07	3.16	1.039	0.69	0.67
April	-0.50	-0.012	0.12	4.41	2.05	1.09	0.53
May	3.39**	0.092	2.20	11.0	7.52	2	0.27
June	1.68	0.036	9.63	16.63	13.73	1.66	0.12
July	3.53**	0.148	13.68	22.54	18.67	2.03	0.12
August	2.89**	0.138	10.44	24.82	16.19	4.57	0.28
September	2.89**	0.068	5.41	13.98	8.25	2.53	0.31
October	2.25*	0.187	0.33	11.91	5.32	3.78	0.71
November	0.75	0.010	0.09	2.94	0.83	0.76	0.91
December	-0.32	-0.001	0	1.76	0.33	0.44	1.33
Spring	1.71	0.018	4.09	14.58	10.61	2.25	0.21
Summer	3.46**	0.084	37.75	63.26	48.58	6.77	0.14
Autumn	2.85**	0.070	6.37	27.4	14.41	6.24	0.43
Winter	0.39	0.002	0.14	2.19	0.85	0.59	0.67
Annual	2.39*	0.02	74.46	52.54	103.80	0.71	0.71

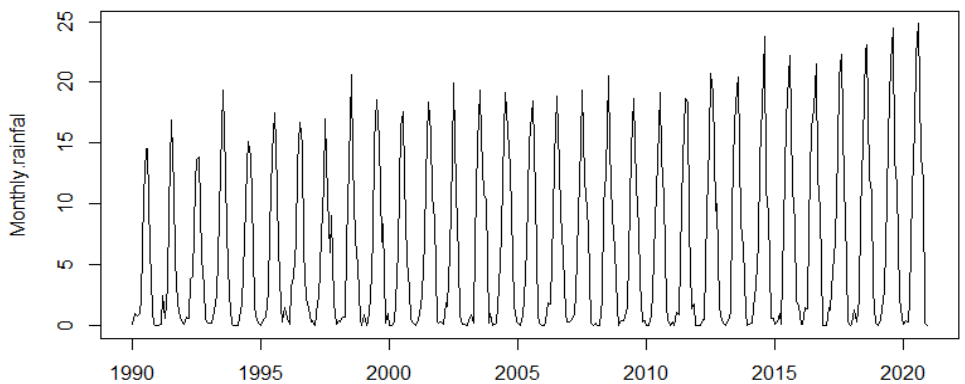

Figure 6 Observed trend of monthly rainfall.

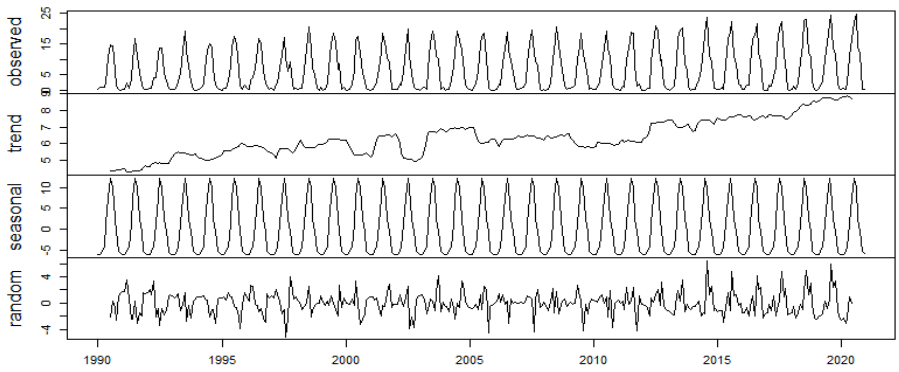

Figure 7 Comparison of observed, random and seasonal tend of monthly rainfall.

In Figure 2, the monthly temperature plot indicates an increasing trend for some months and a decreasing trend for others, providing evidence for rainfall variability within the sub-basin. Along with the MK trend test, the findings of this study are consistent with other studies.

5) Seasonal rainfall trends

The results of the Mann-Kendall (M-K) test showed a positive increasing trend in precipitation for all seasons within the sub-basin, with relatively significant trends detected in summer and autumn (Sens slope (β) values of 0.08 and 0.07 mm/year, respectively). For spring and winter, the Sens slope (β) values were lower at 0.02 and 0.00 mm/year, respectively. The major flooding season (3 to 4 months) had the highest Sens slope β value of 0.11 mm/year, indicating a higher rainfall increase rate compared to other seasons (Table 2). The results of the M-K test, using observed time series of individual seasonal values, are illustrated in Table 2 and Figure 2.

According to Table 2, winter had the highest coefficient of variation (CV) of 67%, followed by autumn with 43%, spring with 21%, and summer with 14%. Winter also had the highest CV of seasonal rainfall during the study period, representing a mean rainfall of 0.85 mm, which was the lowest recorded seasonal rainfall within the study area. These results suggest that seasons with high CV were associated with low seasonal rainfall in the Lake Tana sub-basin, particularly during the dry seasons. Conversely, spring and summer had low CV values and were responsible for generating high rainfall in the study area (Table 2).

Based on the time series plot presented in Figure 9 and 10, it appears that the mean and variance of the series do not vary with the level of the series, indicating stationary. Consequently, additive decomposition was deemed appropriate for separating the time series components. The results of the additive time series decomposition are shown in Figures 8 and 9. The findings revealed an increasing trend in observed random and trend of seasonal rainfall in the study area.

6) Annual rainfall trends

The annual rainfall in the Lake Tana Sub-basin has exhibited increasing trends at a 95% confidence level, as illustrated in Table 2. The Z value of 4.41 is greater than the alpha value of 1.96, indicating statistical significance. In addition, the MK trend test yielded a positive and significant result of 2.39 for the study area. Furthermore, the Sens slope of 0.02 mm/year demonstrates an increasing rate of change in annual rainfall in the study area as depicted in Figure 10 and Table 2.

7) Forecasting of monthly temperature

The study area exhibited both increasing and decreasing trends in monthly temperatures, as indicated by the observed temperature trends. This provided an opportunity to forecast monthly temperatures for the upcoming decade, as illustrated in Figure 11. The figure demonstrates that certain months experienced maximum or minimum temperatures over the past three decades in the study area. The forecasting model predicts a temperature increase for the next 10 years within the study area, as depicted in Figure 16.

The RMSE ARIMA model was found to be the most effective in forecasting climatic variables. Although the forecasting was highly significant for both SNAIVE and ETS models, it was not significant for the ARIMA model at a 95% confidence level (Table 3). However, the root mean square error was used to select the best model for forecasting temperature trends in the study area over the next 10 years, rather than the significance level. This is because the RMSE show the smallest error that the model encounters during forecasting. It also measures the accuracy of the model for predicting future temperature. The ARIMA model had the smallest root mean square error of 1.8889, while the SNAIVE model had the largest error of 2.68 (Table 3).

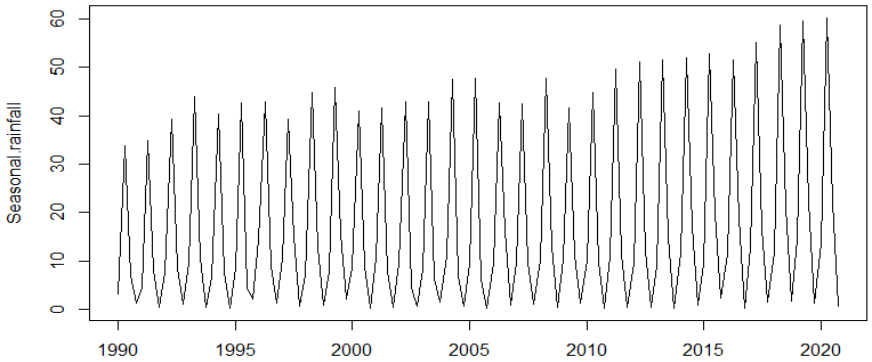

Figure 8 Observed seasonal rainfall trend in the study area.

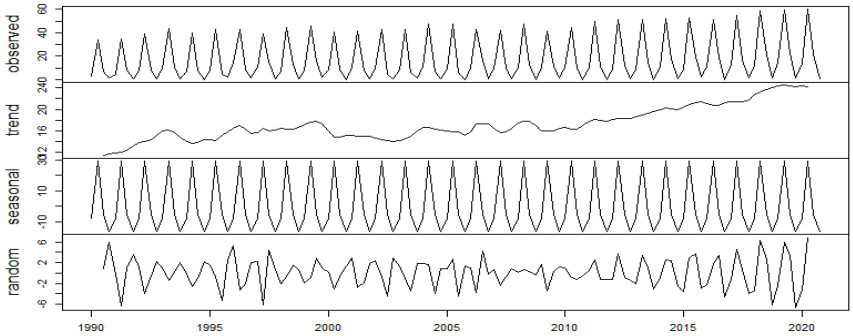

Figure 9 Observed, seasonal and random trend of seasonal rainfall.

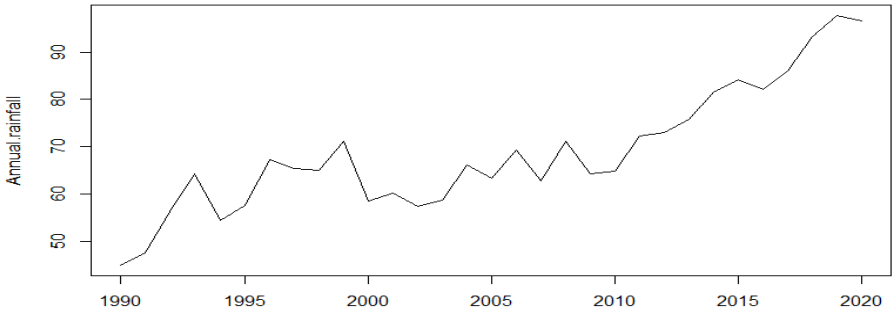

Figure 10 Annual time serious plot of rainfall.

Table 3 Root mean square error for different models

Model type	RMSE	P value
SNAIVE	2.6082	1.187e-12
ETS	1.95209	0.0009492
ARIMA	1.889434	0.4272

The plot reveals notable changes in monthly temperature both in the past and in the future. The differentiated temperature data plot demonstrates that the trend displays seasonality. Figure 12 divides the data into different subgroups to illustrate this pattern. The SNAIVE and ETS models were initially used for comparison with ARIMA for the first forecast. The selection of the best model for forecasting climatic variables was based on the root mean square error, with the model that produced the lowest residual error being selected (Figure 12).

In the graph, the horizontal straight lines represent the mean temperatures for each group (figure 12). The results indicate that each group had a different mean temperature, with the highest maximum temperature being recorded in December and the lowest minimum temperature being recorded in January within the study area. Figure 13 illustrates the seasonal fluctuations in monthly temperature. Based on these fluctuations, the peak temperature was recorded in March and December, while the lowest temperature was observed in April and June.

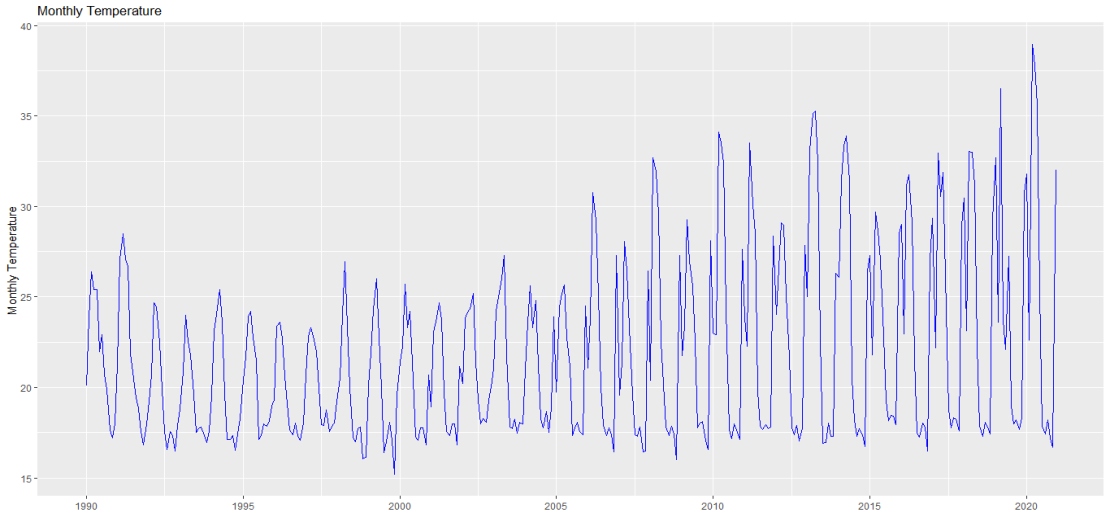

Figure 11 Observed temperature trend in the study area.

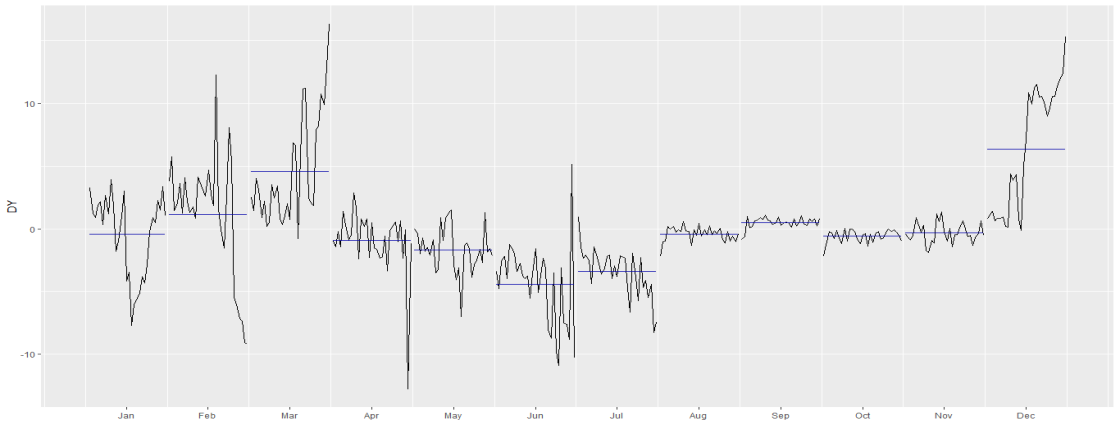

Figure 12 Classifying temperature according to its mean values.

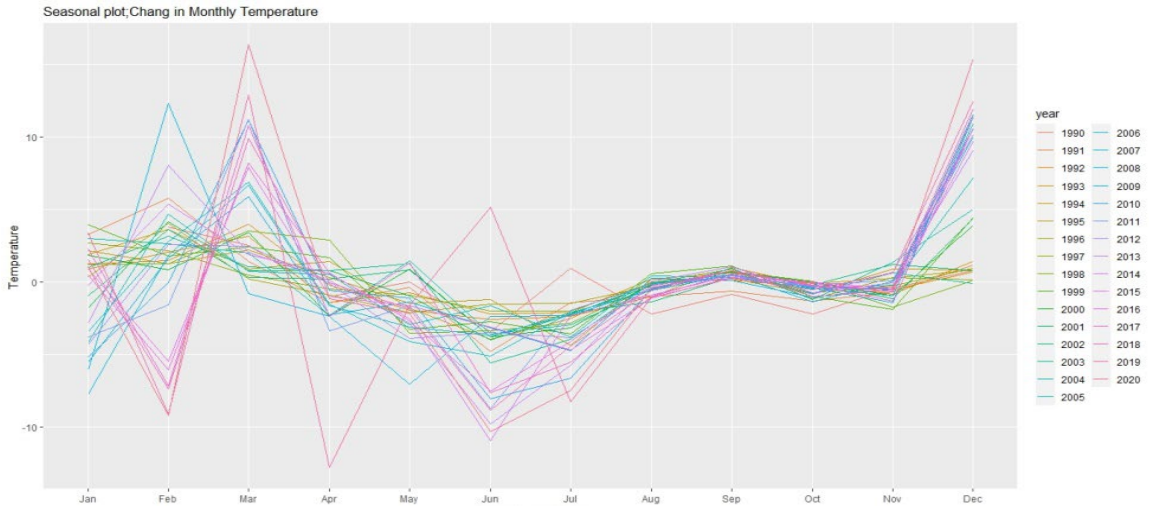

Figure 13 Seasonality of temperature over month

Over the next 10 years, there is a significant increase in monthly temperature in the study area. This rise in temperature, which is linked to climate change, can have adverse impacts on economic activities, ecosystem functions, and human well-being, as evidenced by Figure 14 and Table 4. The graph on the left side of the figure, represented by the pink color, indicates the predicted temperature for the next 10 years in Lake Tana sun basin. The plot of predicted and observed temperatures shows a similar trend, indicating the model's effectiveness.

https://doi.org/10.35762/AER.2024003

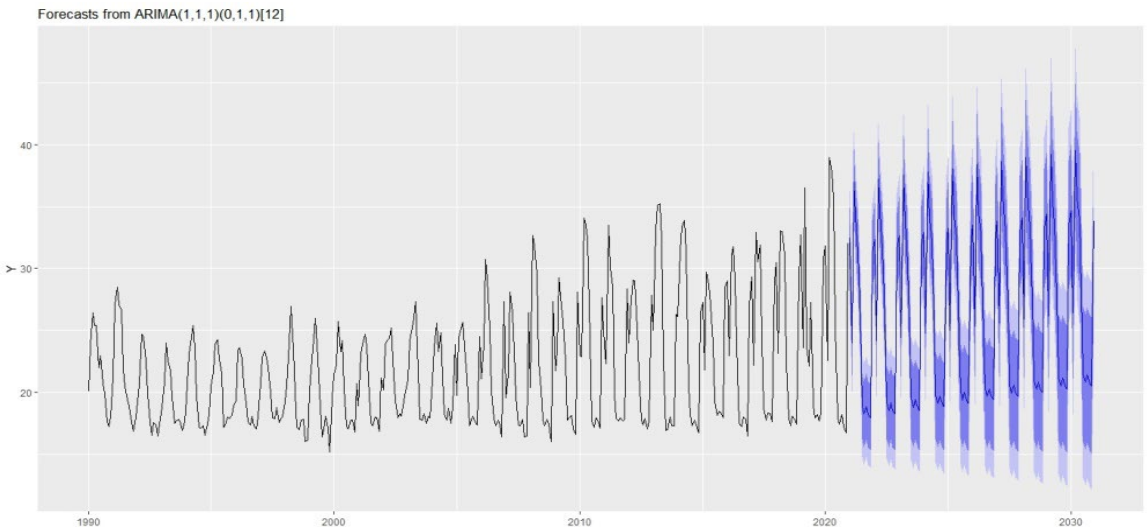

Figure 14 Predicted temperature trend for the coming 10 years in the study area.

Table 4 Predicted mean temperature using ARIMA model

Year	Jan	Feb	Mar	Apr	May	Jun	Jul	Aug	Sep	Oct	Nov	Dec
2021	32.4	24.0	36.98	33.1	31.34	25.61	18.9	18.24	18.85	18.23	17.97	31.24
2022	32.37	24.17	37.22	33.37	31.63	25.89	19.18	18.53	19.14	18.52	18.26	31.53
2023	32.65	24.45	37.51	33.66	31.91	26.18	19.47	18.81	19.42	18.8	18.54	31.82
2024	32.94	24.74	37.79	33.94	32.2	26.47	19.75	19.1	19.71	19.09	18.83	32.1
2025	33.22	25.03	38.08	34.23	32.48	26.75	20.04	19.38	19.99	19.38	19.12	32.39
2026	33.51	25.31	38.36	34.51	32.77	27.04	20.32	19.67	20.28	19.66	19.4	32.67
2027	3.8	25.6	38.65	34.8	33.05	27.32	20.61	19.95	20.57	19.95	19.69	32.96
2028	34.08	25.88	38.94	35.09	33.34	27.61	20.9	20.24	20.85	20.23	19.97	33.24
2029	34.37	26.17	39.22	35.37	33.63	27.9	21.18	20.53	21.14	20.52	20.26	33.53
2030	34.65	26.46	39.51	35.66	33.91	28.18	21.47	20.81	21.42	20.8	20.55	33.82

The findings indicate a growing trend in the mean predicted temperature over time. Moreover, the maximum predicted temperature of 39.91°C was recorded in March, while the minimum of 17.97°C was observed in November, an outcome consistent with the data presented in Table 4. The predicted values suggest that climate change will cause January, April, and May to become increasingly hot, in addition to March. Conversely, June, July, August, September, October, and November will be the coldest months in the future, as illustrated in Figure 14.

8) Forecasting of monthly rainfall

Based on the observed climate data, a shift in rainfall patterns within the Lake Tana Sub-basin is predicted to occur by 2030. This prediction was utilized as a proxy indicator to evaluate the potential impacts of climate change in vulnerability analysis, as presented in Figure 17. The results indicate that the RMSE ARIMA model was the most effective in forecasting climatic variables. While the SNAIVE and ETS models produced highly significant forecasts, the ARIMA model's forecasts were not statistically significant at the 95% level. However, the significance level was not used to determine the optimal model for predicting rainfall, as shown in Table 5.

Table 5 Root mean square error for rainfall using different model

Model type	RMSE	p-value
SNAIVE	2.4279	< 2.2e-16
ETS	1.559838	0.08128
ARIMA	1.548555	0.08777

The observed rainfall trend in the study area displays both increasing and decreasing trends on a monthly basis, allowing for the forecasting of monthly rainfall over the next 10 years. The results indicate significant changes in monthly rainfall patterns, as shown in Figure 15, both in the past and projected for the future. The SNAIVE model was initially used to forecast the first set of data for comparison with the ARIMA model, with the best model for climatic variable forecasting being selected based on the residual error. This is because the RMSE show the smallest error

that the model encounters during forecasting. It also measures the accuracy of the model for predicting future rainfall. Additionally, seasonal fluctuations in monthly rainfall are illustrated in Figure 16.

According to the RMSE analysis, the ARIMA model was found to be the most effective for forecasting climatic variables. In addition, Table 5 displays the residuals of both models, and based on this comparison, the ARIMA model was used to predict monthly rainfall in the study area. The results indicate a significant increase in monthly rainfall over the next 10 years, with the area expected to receive a high amount of rainfall, which could impact various aspects such as economic activities, ecosystem function and human well-being, as depicted in Figure 17. These findings highlight the potential influence of climate change in the study area.

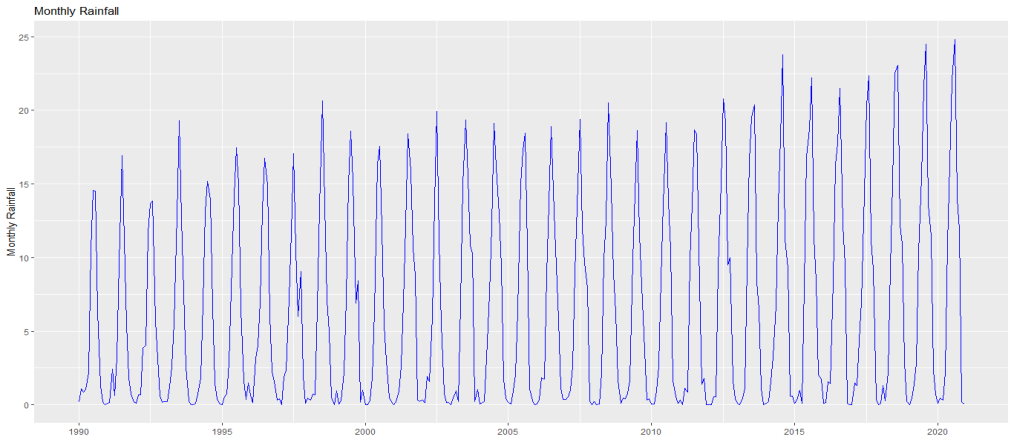

Figure 15 Observed rainfall trend in the study area.

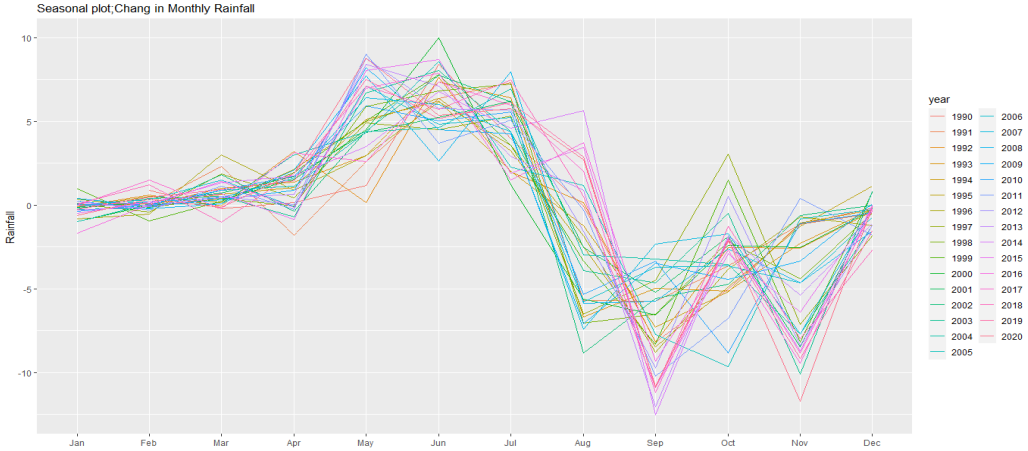

Figure 16 Seasonality of rainfall in the study area.

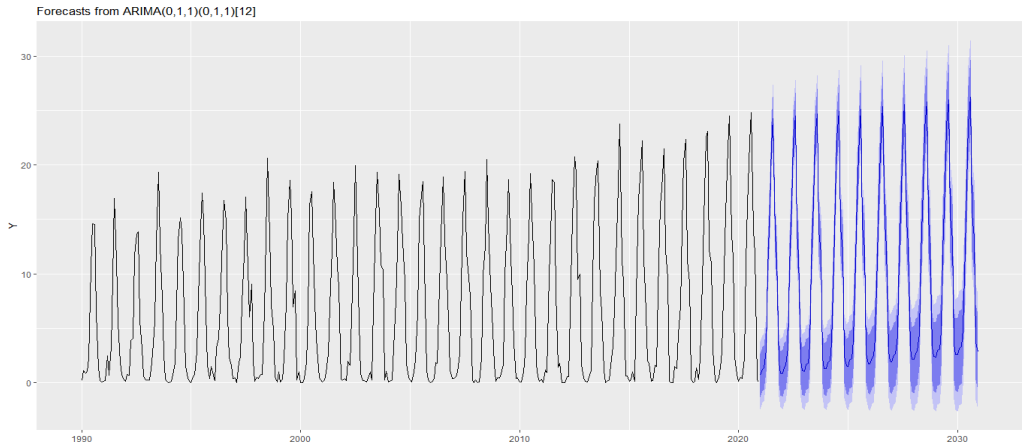

Figure 17 Predicted rainfall trend for the coming 10 years in the study area.

The results of the study reveal that the mean predicted rainfall exhibits an increasing trend over time. Moreover, the maximum predicted rainfall was recorded for August (26.21 mm), while the minimum was recorded for January (0.63mm), which is consistent with the observed data. The predicted values also indicate relatively high

rainfall for May, June, July, August, September and October in the study area, which did not receive significant rainfall in previous years, likely due to climate change. Conversely, January, February, March, November and December were identified as dry months with low levels of rainfall, consistent with the observed data presented in Table 6.

Table 6 Predicted mean for rainfall using ARIMA model for the study area

	Jan	Feb	Mar	Apr	May	Jun	Jul	Aug	Sep	Oct	Nov	Dec
2021	0.63	1.20	1.35	3	10.4	16.25	21.92	24.29	13.51	11.46	1.77	0.86
2022	0.84	1.42	1.57	3.21	10.62	16.46	22.13	24.50	13.72	11.67	1.98	1.08
2023	1.05	1.63	1.78	3.42	10.83	16.67	22.35	24.72	13.94	11.88	2.2	1.29
2024	1.27	1.84	2	3.64	11.04	16.89	22.56	24.93	14.15	12.1	2.41	1.5
2025	1.48	2.06	2.21	3.85	11.26	17.1	22.78	25.15	14.36	12.31	2.62	1.72
2026	1.69	2.27	2.42	4.06	11.47	17.32	22.99	25.36	14.58	12.52	2.84	1.93
2027	1.91	2.48	2.64	4.28	11.68	17.53	23.2	25.57	14.79	12.74	3.05	2.15
2028	2.12	2.7	2.85	4.49	11.9	17.74	23.42	25.79	15.01	12.95	3.26	2.36
2029	2.34	2.91	3.06	4.71	12.11	17.96	23.63	26	15.22	13.17	3.48	2.57
2030	2.55	3.13	3.28	4.92	12.33	18.17	23.84	26.21	15.43	13.38	3.69	2.79

Discussion

The trend analysis of climatic elements within the study area suggests a significant increase in temperature and rainfall, leading to an increase in humidity [17]. The positive Kendall's Z value indicates an upward trend and supports the observation of increasing temperature and rainfall in the Lake Tana Sub-basin over time [31]. Significantly, the p-value is less than the significance level alpha (0.05), confirming the existence of a noticeable trend at a 5% level of significance. These data indicate that there has been a significant increase in temperature, which strongly suggests the impact of climate change on the area [32]. Furthermore, investigating different trend situations for various time intervals reveals that trends may change direction over time and partial trends may need to be examined [33]. This finding is consistent with [34] study of the trends of rainfall and temperature over North-Eastern Nigeria (1949–2014), which showed positive trends ranging from 0.04°C/decade to about 0.001°C/decade. Additionally, the present study aligns with [35] discovery of an increasing trend of temperature and rainfall in Yola, Adamawa State, and Northeastern Nigeria.

These findings are supported by the results of Farooq et al. [36] who found an increasing trend in seasonal temperatures in Kazakhstan between 1970–2017 using non-parametric statistical methods and GIS technologies. Furthermore, Frimpong et al. [37] reported similar results of an increasing seasonal and annual temperature trend in the Accra and Kumasi metropolises in Ghana. Similarly, Khyber et al. [38] found an increasing trend in annual temperature in Dramaga Sub-District, Bogor, Indonesia, and used it as a proxy indicator for exposure to future climate change in vulnerability analysis.

The trend analysis of seasonal temperature reveals fluctuations in temperature within each season, suggesting that there are changes in climate and weather conditions in the study area [39]. The monthly and seasonal temperature and rainfall display varying coefficients of variation, signifying that seasonal temperature is highly variable over time, which suggests the existence of climate change in the study area [40]. The positive Sens slope of seasonal temperature indicates an increasing rate of seasonal temperature in the study area, highlighting that the weather conditions of the sub-basin are worsening for human beings [41]. These findings are consistent with those of Ceribasi et al. [42] who observed an increasing trend in annual mean temperature in both basins (Susurluk and Van Lake Closed Basins), leading to climate change in these areas.

The trend analysis of annual temperature and rainfall displays a fluctuating trend, indicating changes in the climate and weather conditions in the study area [31]. The positive and significant value of Z confirms an increasing trend in temperature and rainfall within the study area, which implies the existence of climate change and variability [43]. These findings are consistent with Afrira-Yampah et al. [44] report of higher rainfall levels in September and October and lower rainfall levels in January, December, and February. The rate of change in temperature and rainfall was positive and increasing due to the positive value of Sens slope. This result aligns with Cui et al. [45] who reported the

significantly increasing of annual maximum, minimum, and mean temperatures at rates ranging from 0.15°C/10yr to 0.23°C/10yr over the whole study area during 1960-2015 in the Yangtze River Basin, China. Furthermore, Cicek et al. [46] identified seven stations that displayed increasing precipitation trends in all seasons clustered in the Black Sea coastal belt and North-eastern Anatolia, which is consistent with the present study's results.

Given the strong trend and fluctuation observed in the data series for monthly, seasonal, and annual temperature and rainfall in the study area, it is possible to apply the predicting model ARIMA. This finding is similar to Bagirov et al. [47] who reported high variability in predicted temperature and rainfall using seven different models, which causes climate change in Victoria, Australia. The means of predicted values for temperature and rainfall indicate an increasing trend for the next 10 years, which suggests that the climate condition in the area will be very fragile in the future. These findings suggest that the area will be more affected due to climate change resulting from fluctuations in major climatic variables, especially temperature and rainfall. This result is consistent with the study of Bari et al. which found that ARIMA was used to compare observed and forecasted values with a 95% confidence limit and reported an increasing trend in future temperature and rainfall in Sylhet City, Bangladesh. This result is consistent with Gizachew and Shimelis [49] who also found a projected increase in temperature and rainfall by 2050 in the Central Rift Valley of Ethiopia. Additionally, Dankwa et al. [21] reported comparable findings regarding the analysis and forecasting of rainfall patterns in the Manga-Bawku area of northeastern Ghana.

Conclusion and recommendation

The study's findings suggest that there is a positive and significant trend in monthly, seasonal, and annual temperature and rainfall in the study area. According to the MK trend analysis, it can also be concluded that March is the hottest month, and spring is the hottest season. Furthermore, the rate of change in temperature and rainfall was positive and increasing for monthly, seasonal, and annual periods. These results indicate the presence of climate variability and change within the study area. The study's findings indicate that the ARIMA model is the most effective in forecasting future temperature and rainfall, as it has the smallest RMSE. The predicted mean values of temperature and rainfall show an increasing trend, which is similar to the observed data. These results suggest that climate change is likely to exacerbate in the study area due to the increasing temperature and rainfall. The study's findings suggest that the Lake sub-basin is currently experiencing severe climate change, which is projected to continue based on the predicted values of temperature and rainfall. To address this issue, various adaptation and mitigation measures, such as afforestation, buffering of the lake, and changes in lifestyle, should be implemented by the government, policy-makers, and other relevant organizations. It's also better to conduct additional research to see the effect of current and future climate change on agriculture ecosystem function and socio-economic activities in the study area.

Reference

[1] Bogale, G.A., Tolossa, T.T. Climate change intensification impacts and challenges of invasive species and adaptation measures in Eastern Ethiopia. Sustainable Environment, 2021, 7(1), 1–25.

[2] IPCC, Climate Change 2021 The physical science basis aummary for policymakers. 2021.

[3] Qu, M., Wan, J., Hao, X. Analysis of diurnal air temperature range change in the continental United States. Weather and Climate Extremes, 2014, 4, 86–95.

[4] IPCC, Climate change 2013. Edited by. 2013.

[5] Kjellstrцm, E., Thejll, P., Rummukainen, M., Christensen, J.H. Emerging regional climate change signals for Europe under varying large-scale circulation conditions. Climate Research, 2013, 56(May 2014), 103–119.

[6] Luoto, T.P., Nevalainen, L. Long-term water temperature reconstructions from mountain lakes with different catchment and morphometric features. Scientific Reports, 2013, 3, 2488.

[7] Holsinger, L., Keane, B., Eby, L. Impacts of climate change and wildfire on stream temperature and bull trout in the East Fork Bitterroot River, 2012.

[8] UNFCCC, Cimate change: Impacts, impacts, vulnerabilities and adaptation in developing countries. 2007.

[9] IPCC, Climate change 2014 synthesis report. 2014.

[10] Chinwe, I.S. Resilient Adaptation to climate change in African agriculture, 2010, 54.

[11] Murat, Trend and homogeneity analysis in temperature and rainfall series in western Black Sea region, Turkey. Theoretical and Applied Climatology, 2020, 139(3–4), 837–848.

[12] Norbert, G., Guedes, M., De Moraes, A. Decision support for the (inter-) basin management of water resources using integrated hydro-economic modeling. Hydrology, 2021, 8(42), 1–19.

[13] Gadedjisso-tossou, A., Adjegan, K.I.I. Rainfall and temperature trend analysis by Mann–Kendall test and significance for rainfed cereal yields in Northern Togo. Science, 2021, 3(17), 1–20.

[14] Panda, A., Sahu, N. Trend analysis of seasonal rainfall and temperature pattern in Kalahandi, Bolangir and Koraput districts of Odisha, India. Atmospheric Science Letters, 2018, September. 1–10, 2019.

[15] Ragatoa, D.S., Ogunjobi, K.O. A trend analysis of temperature in selected stations in Nigeria using three different approaches. Open Access Library Journal, 2018, 5, 1–18.

[16] Getachew, B., Manjunatha, B.R. Climate change projections and trends simulated from the CMIP5 models for the Lake Tana sub-basin, the Upper Blue Nile (Abay) River Basin, Ethiopia. Environmental Challenges, 2021, 5(August), 100385.

[17] Alemu, Z.A., Dioha, M.O. Climate change and trend analysis of temperature: the case of Addis Ababa, Ethiopia. Environmental Systems Research, 2020, 9(1), 1–15.

[18] Getahun, Y.S., Li, M.H., Pun, I.F. Trend and change-point detection analyses of rainfall and temperature over the Awash River basin of Ethiopia. Heliyon, 2021, 7(9), e08024.

[19] Gourdji, S.M., Sibley, A.M., Lobell, D.B. Global crop exposure to critical high temperatures in the reproductive period: Historical trends and future projections. Environmental Research Letters, 2013, 8(2), 1–11.

[20] Narayanan, P., Basistha, A., Sarkar, S., Kamna, S. Trend analysis and ARIMA modelling of pre-monsoon rainfall data for western India. Comptes Rendus Geoscience, 2013, 345(1), 22–27.

[21] Dankwa, P., Cudjoe, E., Amuah, E.E.Y., Kazapoe, R.W., Agyemang, E.P. Analyzing and forecasting rainfall patterns in the Manga-Bawku area, northeastern Ghana: Possible implication of climate change. Environmental Challenges, 2021, 5(July), 100354

[22] Kaur, J., Parmar, K.S., Singh, S. Autoregressive models in environmental forecasting time series: a theoretical and application review. Environmental Science and Pollution Research, 2023, 30(8), 19617–19641.

[23] CSA. 2007 population and housing census of administrative, 2012.

[24] Goshu, G., Aynalem, S., Problem overview of the Lake Tana Basin. 2017.

[25] Dersseh, A.A.K., Kibret, A.A., Tilahun, S.A., Worqlul, A.W., Moges, M.A., Dagnew, D.C., …, Melesse, A.M. Potential of water hyacinth infestation on Lake Tana, Ethiopia: A prediction using a GIS-based multi-criteria technique. Water, 2019, 11(9), 1921, 1–17.

[26] Fick, S.E., Hijmans, R.J. WorldClim 2: New 1-km spatial resolution climate surfaces for global land areas. International Journal of Climatology, 2017, 4315(May), 4302–4315.

[27] Hamed, K., Gachon, P. Exact distribution of the Mann- Kendall trend test statistic for persistent data. Journal of Hydrology, 2009, 365, 86–94.

[28] Basin, Y.R., Yang, R. Spatio-Temporal variability in hydroclimate over the upper. Atmosphere. 2022, 13(317), pp. 1–34, 2022.

[29] Klasson, K.T. Using excel for dynamic analysis of variance and unplanned multiple comparisons procedures, 2020, USDA.

[30] Sen, P.K. Estimates of the Regression Coefficient Based on Kendall' s Tau Pranab Kumar Sen. Journal of the American Statistical Association, 1968, 63(324), 1379–1389.

[31] Mateus, C., Potito, A. Long-term trends in daily extreme air temperature indices in Ireland from 1885 to 2018. Weather and Climate Extremes, 2022, 36(May), 100464.

[32] El Kasri, J., Lahmili, A., Soussi, H., Jaouda, I., Bentaher, M. Trend analysis of meteorological variables: Rainfall and temperature. Civil Engineering Journal, 2021, 7(11), 1868–1879.

[33] Li, J., Li, Z.L., Wu, H., You, N. Trend, seasonality, and abrupt change detection method for land surface temperature time-series analysis: Evaluation and improvement. Remote Sensing of Environment, 2022, 280(January), 113222.

[34] Hassan, S.F., Tantawi, A.M.E.-, Hashidu, U.S. Trends of rainfall and temperature over North-Eastern Nigeria (1949-2014). IOSR Journal of Environmental Science, Toxicology and Food Technology 11(05), 01–09.

[35] Oyerinde, O.O. Analysis of decadal rainfall and temperature trend in Warri, Nigeria. European Journal of Environment and Earth Sciences, 2021, 2(2), 15–18.

[36] Farooq, I., Shah, A.R., Salik, K.M., Ismail, M. Annual, seasonal and monthly trend analysis of temperature in Kazakhstan During 1970–2017 using non-parametric statistical methods and GIS technologies. Earth Systems and Environment, 2021, 5(3), 575–595.

[37] Frimpong, B.F., Koranteng, A., Molkenthin, F. Analysis of temperature variability utilising Mann–Kendall and Sen's slope estimator tests in the Accra and Kumasi Metropolises in Ghana.

Environmental Systems Research, 2022, 11(1), 1–13.

[38] Khyber, E., Syaufina, L., Sunkar, A. Variability and time series trend analysis of rainfall and temperature in Dramaga Sub-District, Bogor, Indonesia. IOP Conference Series: Earth and Environmental Science, 2021, 771(1), 012016.

[39] Panwar, M., Agarwal, A., Devadas, V. Analyzing land surface temperature trends using non-parametric approach: A case of Delhi, India. Urban Climate, 2018, 24(November 2017), 19–25.

[40] Mahmood, R., Jia, S., Zhu, W. Analysis of climate variability, trends, and prediction in the most active parts of the Lake Chad basin, Africa. Scientific Reports, 2019, 9(1), 1–18.

[41] Siddiqui, A., Kushwaha, G., Nikam, B., Srivastav, S.K., Shelar, A., Kumar, P. Analysing the day/ night seasonal and annual changes and trends in land surface temperature and surface urban heat island intensity (SUHII) for Indian cities. Sustainable Cities and Society, 2021, 75, (August), 103374.

[42] Ceribasi, G., Aytulun,,U. Investigation of the effect of climate change on precipitation and temperature data of Susurluk Basin and Van Lake closed basin. International Journal of Global Warming, 2020, 22(1), 54–71.

[43] Panda, A., Sahu, N. Trend analysis of seasonal rainfall and temperature pattern in Kalahandi, Bolangir and Koraput districts of Odisha, India. Atmospheric Science Letters, 2019, 20, 10, 1–10.

[44] Afrira-Yampah, E., Saeed, B.I.I., Karim, A. Sarima modelling and forecasting of monthly rainfall in the Brong Ahafo Region of Ghana. World Environment, 2016, 6(1), 1–9.

[45] Cui, L., Wang, L., Lai, Z., Tian, Q., Liu, W., Li, J. Innovative trend analysis of annual and seasonal air temperature and rainfall in the Yangtze River Basin, China during 1960–2015. Journal of Atmospheric and Solar-Terrestrial Physics, 2017, 164(July), 48–59.

[46] Cicek, I., Duman, N. Seasonal and annual precipitation trends in Turkey Ihsan. Carpathian Journal of Earth and Environmental Sciences, 2015, 10(20), 77–84.

[47] Bagirov, A.M., Mahmood, A., Barton, A. Prediction of monthly rainfall in Victoria, Australia: Clusterwise linear regression approach. Atmospheric Research, 2017, 188, 20–29.

[48] Bari, S.H., Rahman, M.T., Hussain, M.M., Ray, S. Forecasting monthly precipitation in Sylhet city using Arima model. Civil and Environmental Research, 2015, 7(1), 69–78.

[49] Gizachew, L., Shimelis, A. analysis and mapping of climate change risk and vulnerability in central rift valley of Ethiopia climate change is one of the current issues that severely impact all climate sensitive sectors like agriculture. The manifesttation of climate change such as. African Crop Science Journal, 2014, 22(Vi), 807–818.